Phytomedicine 22 (2015) 77–85

Contents lists available at ScienceDirect

Phytomedicine

journal homepage: www.elsevier.com/locate/phymed

Sesqui- and triterpenoids from the liverwort *Lepidozia chordulifera* inhibitors of bacterial biofilm and elastase activity of human pathogenic bacteria

M. Gilabert[a,b,*], K. Marcinkevicius[a], S. Andujar[c], M. Schiavone[d], M.E. Arena[a,b], A. Bardón[b]

[a] INQUINOA-CONICET, Ayacucho 471, 4000 Tucumán, Argentina
[b] Facultad de Bioquímica, Química y Farmacia, Universidad Nacional de Tucumán (UNT), Ayacucho 471, 4000 Tucumán, Argentina
[c] Facultad de Química, Bioquímica y Farmacia, Universidad Nacional de San Luís (UNSL), Ejército de Los Andes 950, 5700 San Luis, Argentina
[d] Facultad de Ciencias Naturales e Instituto Miguel Lillo, Universidad Nacional de Tucumán, Miguel Lillo 251, Tucumán 4000, Argentina

ARTICLE INFO

Article history:
Received 26 June 2014
Revised 19 August 2014
Accepted 15 October 2014

Keywords:
Lepidozia chordulifera
Biofilm
Elastase
Pseudomonas aeruginosa
Staphylococcus aureus

ABSTRACT

Five dammarane-type triterpenoids, five pentacyclic triterpenoids (three of them carrying a carboxylic acid group), and two aromadendrane-type sesquiterpenoids were isolated from an Argentinian collection of the liverwort *Lepidozia chordulifera*. Compounds were characterized by comparison of their spectral data with those previously reported and tested in their ability to control bacterial growth, biofilm formation, bacterial Quorum Sensing process (QS), and elastase activity of *Pseudomonas aeruginosa*, as well as bacterial growth and biofilm formation of *Staphylococcus aureus*. The key role played by biofilm and elastase activity in bacterial virulence make them a potential target for the development of antibacterial agents. The aromadendrane-type sesquiterpenoid viridiflorol was the most potent biofilm formation inhibitor, producing 60% inhibition in *P. aeruginosa* and 40% in *S. aureus* at 50 μg/ml. Ursolic and betulinic acids (two of the pentacyclic triterpenoids isolated) were able to reduce 96 and 92% the elastase activity of *P. aeruginosa* at 50 μg/ml, respectively. Among the analyzed triterpenoids, those that carry a dammarane skeleton were the most potent inhibitors of the *P. aeruginosa* biofilm formation and were active against both *P. aeruginosa* and *S. aureus*. Subsequently, a computer-assisted study of the triterpenoid compounds was carried out for a better understanding of the structure-activity relationships.

Introduction

The genus *Lepidozia* belonging to the Porellaceae family of the Class Hepaticae (liverworts) is mainly distributed in tropical and subtropical regions of the southern hemisphere and its species are rich sources of various types of secondary metabolites including isobicyclogermacranes, lepidozanes, cadinanes, eudesmanes, maalianes, vitranes, and bibenzyls (Asakawa et al., 2012). *Lepidozia chordulifera* is a light green to green-brown plant that grows over rocks, trees, and soil forming loose tufts (Ardiles et al., 2008). The only previous chemical investigation of a Chilean collection of *L. chordulifera* revealed that triterpenoids represented the major constituents of the dichloromethane extract in which 21,28-epoxy-18β,21β-dihydroxybaccharan-3-one, taraxerol, shoreic, betulinic, betulonic, and ursolic acids were present (Zapp et al., 2008).

Bacterial biofilms are complex communities of bacteria embedded in a self-produced matrix and attached to inert or living surfaces (Costerton et al., 1999). These microorganisms are more resistant to antibiotics and to the immunologic system than planktonic cells (Stewart and Costerton, 2001). Processes of biofilm formation, virulence factors production, and resistance to antimicrobials are regulated by the Quorum Sensing (QS) process, a bacterial communication system mediated by diffusible chemical signals called autoinducers (van Delden and Iglewski, 1998). Sesquiterpene lactones, fusicoccane-type diterpenoids, annonaceous acetogenins, and acylphloroglucinols from plants are able to alter biofilm formation of *Pseudomonas aeruginosa* (Cartagena et al., 2007; Gilabert et al., 2011) and *Staphylococcus aureus* (Arena et al., 2011; Socolsky et al., 2010), as well as the production of some virulence factors of *P. aeruginosa* such as elastase (Amaya et al., 2012). *Pseudomonas* elastase, also known as pseudolysin or LasB, is a metalloprotease that has long been recognized as a key

* Corresponding author at: Universidad Nacional de Tucumán, Ayacucho 471, 4000 San Miguel de Tucumán, Argentina. Tel.: +54 381 4247752x7062; fax: +54 381 4248169.
E-mail address: mgilabert@fbqf.unt.edu.ar, gilabertmiguel@gmail.com (M. Gilabert).

http://dx.doi.org/10.1016/j.phymed.2014.10.006
0944-7113/

virulence factor produced by *P. aeruginosa* (Stewart and Costerton, 2001). The secreted protease degrades a broad range of host tissue proteins and key biomolecules involved in innate immunity such as inmunoglobulins, complement factors, and cytokines (Liu, 1974). In addition, LasB acts within the bacterial cell as a key regulator in the generation of the secreted polysaccharides that constitute the bacterial biofilm (Cathcart et al., 2009). Inhibition of one of the main virulence factors (elastase) of bacteria turn them susceptible to the attack of the host immune system. Thus, LasB inhibition by natural products could be an important strategy for controlling *Pseudomonas* virulence in bacterial infections (Sokol et al., 2000).

Herein we report the ability of ten *L. chordulifera* terpenoids (**1**–**10**) to control bacterial growth, biofilm formation, QS process, and elastase activity of *P. aeruginosa*, as well as, bacterial growth and biofilm formation of *S. aureus*.

Experimental

General

NMR spectra were recorded on a Bruker spectrometer operating at 300 MHz for ^{1}H and 75 for ^{13}C with TMS as internal standard in $CDCl_3$. For preparative HPLC a Gilson chromatograph with refractive index detector was used. HPLC columns: (A) Chemo Pack Develosil 60 (5 μm, 10 mm i.d. × 250 mm), (B) Phenomenex Luna C18 (5 μm, 10 mm i.d. × 250 mm), and (C) Phenomenex Luna C8 (5 μm, 10 mm i.d. × 250 mm).

Plant material

L. chrodulifera, growing over rocks and trees was collected in February 2009 in Lago Steffen, Rio Negro province, Argentina. A voucher specimen (LIL N° 3414) is deposited at the Herbarium of Fundación Miguel Lillo, Tucumán, Argentina.

Extraction and isolation

The air-dried plant material (240 g) was extracted at room temperature for 7 days with diethyl ether (Et_2O), in a shaker, to give 5.9 g of residue after solvent removal (yield 2.46%). The extract was subjected to Sephadex LH20 CC (MeOH–CH_2Cl_2, 1:1) to get rid of chlorophylls, and then to silica gel CC with *n*-hexane with increasing amounts of EtOAc (0–100%), and finally MeOH as eluents, to give five fractions (I–V).

Fr I (370 mg) was submitted to HPLC (Column A, *n*-hexane-EtOAc, 49:1) to give compound **1** (17 mg). Fr II (103 mg) was a mixture further separated by HPLC (Column A, *n*-hexane-EtOAc, 26:1) to yield compounds **2** (34 mg), **11** (10 mg), and **12** (15 mg). Fr III (80 mg) was processed by RP-HPLC (Column B, MeOH–H_2O, 9:1) to give compound **8** (7 mg). RP-HPLC (Column B, MeOH–H_2O, 17:1) of Fr IV (150 mg) yielded compounds **9** (3 mg), **10** (4 mg) and a mixture that was reprocessed by RP-HPLC using column C (MeOH–H_2O, 17:1 + 1% Acetic acid) to obtain compounds **3** (11 mg), **4** (3 mg), and **5** (6 mg). Fr V (150 mg) was submitted to Sephadex LH20 CC (MeOH–CH_2Cl_2, 1:1) and then to RP-HPLC (Column B, MeOH–H_2O, 22:3 + 1% acetic acid) to give **6** (14 mg) and a mixture submitted to RP-HPLC with column C (MeOH–H_2O, 21:4 + 1% Acetic acid) to obtain **7** (3 mg) and a new portion of **6** (3 mg). Purity and chemical structures were assessed by HPLC (single peaks in the chromatogram) and spectroscopic data which were compared with those previously reported.

Tests

Compounds **2**–**11** were tested on their ability to alter bacterial growth, biofilm formation, Quorum Sensing process, and elastase activity of *P. aeruginosa* as well as the bacterial growth and biofilm formation of *S. aureus*. Compound **1** (taraxerone) underwent partial decomposition therefore it could not be tested, while compound **12** (*ent*-spathulenol) had been previously evaluated (Gilabert et al., 2011).

Microorganisms

Pseudomonas aeruginosa ATCC 27853 (Gram negative bacilli) and *Staphylococcus aureus* ATTC 6538 P (Gram positive cocci) strains were selected for the bioassays.

Bacterial growth

An overnight culture of *P. aeruginosa* ATCC 27853 was diluted to reach an OD 0.125 ± 0.02 at 560 nm in Luria–Bertani (LB) medium. An overnight culture of *S. aureus* ATTC 6538 P was diluted to reach an OD 0.13 ± 0.03 at 560 nm in Mueller Hinton medium. The diluted cultures (190 μl) were placed in each of the 96 wells of a microtitre polystyrene plate. Solutions containing 1 and 0.1 mg/ml of compounds **2**–**11** in DMSO/distilled water (1:1) were prepared separately and 10 μl of each were pipetted to the plastic microtitre plate wells individually (8 replicates). Control growth wells (8 replicates) contained the diluted culture (190 μl) and 10 μl of a solution of DMSO/water (1:1) in which the final concentration of DMSO is 2.5%. Ciprofloxacin, a known biofilm inhibitor, was incorporated to the bioassay at 5 μg/ml in the same experimental conditions employed to evaluate the compounds (8 replicates). At this concentration, ciprofloxacin inhibited the biofilm formation but did not modify significantly the bacterial growth (Sandasi et al., 2011). After 24 h incubation at 37 °C, bacterial growth was detected as turbidity (560 nm) using a microtitre plate reader (Power Wave XS2, Biotek, VT, USA). Control absorbance values were 1.59 for *P. aeruginosa* and 1.35 for *S. aureus*.

Biofilm formation assay

For biofilm quantification, a micro method based on a protocol previously reported was employed (O'Toole and Kolter, 1998). Biofilms formed after 24 h incubation of bacterial cultures prepared as described in the previous paragraph, were stained with 20 μl of an aqueous solution of crystal violet (0.1%, w/v) for 20 min. After washing with water, the liquid was discarded from the wells and the material that remained fixed to the polystyrene (containing biofilm) was washed with PBS (thrice). Crystal violet bound to biofilm was removed from each well employing 200 μl absolute ethanol during 30 min at 37 °C with shaking. Absorbance (560 nm) of ethanol solutions of crystal violet was determined using a microtitre plate reader (Power Wave XS2, Biotek, VT, USA). Wells containing ciprofloxacin at 5 μg/ml were employed as a positive control of biofilm formation. Control growth wells treated as described above were employed as a control for biofilm formation. Absorbance values were 2.09 for *P. aeruginosa* and 0.35 for *S. aureus*.

Screening for Quorum sensing inhibition

An overnight culture of the reporter strain *P. aeruginosa* qsc 119 (Whiteley et al., 1999), grown at 37 °C in LB, was diluted 10 times in the same medium. A 100 μl portion of this suspension was mixed, in each microplate well, with 100 μl cell-free culture supernatant obtained from *P. aeruginosa* ATCC 27853 cultured in LB media containing 50 and 5 μg/ml of compounds **2**–**11**, during 24 h. Azithromycin, known to interfere with the QS process (Tateda et al., 2001) was used at 5 μg/mL as QS inhibition positive control under the same experimental conditions as for compounds **2**–**11**. Quorum sensing control wells (eight replicates) contained

cell-free culture supernatant (100 μl) obtained from *P. aeruginosa* ATCC 27853 cultured in LB media with 10 μl of DMSO/water (1:1).

P. aeruginosa qsc 119 is a mutant that cannot produce its own autoinducers (QS signal molecules), which in the case of Gram (−) bacteria (*P. aeruginosa* is one of them) are known as acyl homoserine lactones (AHL). However, *P. aeruginosa* qsc 119 responds to exogenous AHL molecules by the production of ß-galactosidase. As a consequence, ß-galactosidase activity is under QS-control and in direct relationship with the autoinducers (AHL) activity. ß-Galactosidase activity was measured spectrophotometrically by the Miller test (O'Toole and Kolter, 1998). Quorum sensing control activity was 13.8 expressed as Miller units.

Elastase B activity

Elastolytic activity was determined using a modification of a previously reported method (Caballero et al., 2001). Elastin Congo red (100 μl) (Sigma) dissolved in Tris–HCl (pH 8.0) at a concentration of 5 mg/ml was mixed with 100 μl cell-free culture supernatant from *P. aeruginosa* ATCC 27853 grown, during 24 h, in LB media containing 50 and 5 μg/ml of compounds **2**–**11**. The reaction mixture (200 μl) was incubated at 37 °C for 24 h and centrifuged at 13,000 rpm for 10 min. The absorbance (495 nm) of the supernatant is a measure of the *elastase B* activity.

Statistical analysis

Data are presented as mean ± S.D. The statistical significance of differences between mean values was evaluated by *Dunnett*'s test. A value of $p \leq 0.05$ was considered significant.

Calculation methods for the computer-assisted conformational and electronic study of triterpene compounds

In a preliminary and exploratory step, the conformational study of dammarane compounds (**6**–**9**) was carried out from a simple scan of the torsional angle θ (C13–C17–C20–O, Fig. 1) using semiempirical PM6 calculations with GAUSSIAN 03 software. To obtain the potential energy curves (PECs) the torsional angle θ was rotated 360° every 30°. Although the semi-empirical calculations can define broad conformational features, a more accurate method such as DFT calculations should be employed to make sure that the molecular flexibility and relative stability of the conformers are correct. Thus, DFT [B3LYP/6-31G(d)] calculations were performed to confirm the preliminary results. Subsequently, DFT (B3LYP/6-31G(d)) calculations were used in the geometry optimization jobs for the minimum value already obtained.

Once the energetically preferred form of the triterpene compounds (**1**–**9**) was determined, an electronic analysis using molecular electrostatic potentials (MEPs) was performed. Surfaces were generated using a B3LYP/6-311 + +G(d and p) single point calculation from the MOLEKEL program. The electrostatic potential is the energy of interaction of a positive point charge with the nuclei and electrons of a molecule. The MEP coloring represents electrostatic potential with red indicating the strongest attraction to the positive point charge and blue indicating the strongest repulsion. MEPs have shown to provide representative measure of overall molecular charge distribution as well as reliable information, both, on the interaction sites of the molecules with point charges and on the comparative reactivities of these sites (Politzer and Truhlar, 1981).

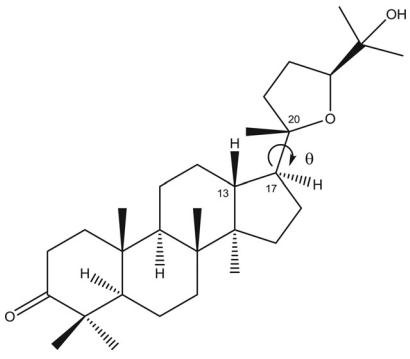

Fig. 1. Compound **8** showing the torsional angle θ (C13–C17–C20–O).

Results

From an Argentinian collection of *L. chordulifera*, the triterpenoids **1–10** and the aromadendrane sesquiterpenoids **11–12** were isolated. Compounds **1** and **2** were identified as the pentacyclic triterpenes taraxerone and taraxerol based on their spectroscopic features and previously reported data (Hernandez-Chavez et al., 2012). Constituents **3**, **4**, and **5** were identified as oleanolic, ursolic, and betulinic acids by comparison of their spectral data with those previously reported for the authentic compounds (Gohari et al., 2009; Ayatollahi et al., 2011; Muhit et al., 2010). A bibliographic inspection of the ^{1}H and ^{13}C NMR spectroscopic data of the carboxylic acids **3**, **4**, and **5** showed very dissimilar data, particularly for compound **4** (ursolic acid) (Ayatollahi et al., 2011; Güvenalp et al., 2009; Morales-Serna et al., 2011), with chemical shifts given for solvent mixtures. In Table 1, our comparative values of diagnostic signals for compounds **3**, **4**, and **5** in $CDCl_3$ are presented. Compounds **6**, **7**, **8**, **9**, and **10** were identified as the dammaranes shoreic acid (Govindachari et al., 1994), eichlerialactone (Singh and Aalbersberg, 1992), cabraleone, cabraleadiol (Hisham et al., 1996), and 3ß-hydroxynordammaran-20-one (Tanaka et al., 1987) based on their spectroscopic features and by comparison with literature data. Comparative ^{1}H NMR data for dammaranes **6**–**9** are presented in Table 2. The relative stereochemistry of the lateral chain carrying the THF group on C-17 and the relative stereochemistry of the isopropylol group on C-24 of compounds **6**, **8**, and **9**, were established as depicted based on the chemical shifts of H-24 in the ^{1}H NMR spectrum. In compounds **6**, **8** and **9**, the H-24 signal appears as a double doublet at δ_H 3.65, while their epimers (eichlerianic acid, ocotillone, and ocotillol) show this signal as a triplet at δ_H 3.71 (Hisham et al., 1996). Compounds **11** and **12** were identified as the aromadendrane sesquiterpenoids viridiflorol (Bombarda et al., 2001) and *ent*-spathulenol (Asakawa et al., 2012; Gilabert et al., 2011) by comparison of their spectral data with those previously reported.

Taraxerol (**2**), ursolic (**4**), betulinic (**5**), and shoreic (**6**) acids, and 3ß-hydroxynordammaran-20-one (**10**) were also isolated in a previous investigation of *L. chordulifera* (Zapp et al., 2008). Furthermore, taraxerone (**1**), taraxerol (**2**), ursolic acid (**4**), and betulinic acid (**5**) were previously reported from *L. raptans* (Zhang, 2011). Cabraleadiol (**9**) was previously isolated from the liverwort *Blepharidophyllum densifolium* (Flegel and Becker, 1999) while viridiflorol (**11**) was obtained from *Bazzania trilobata*, *Locopholea bidentata*, and *L. heterophylla* (Asakawa et al., 2012). The present is the first report on the occurrence of oleanolic acid (**3**), eichlerialactone (**7**), and cabraleone (**8**) in liverworts.

Despite triterpenes are widely distributed throughout the plant kingdom, especially in higher plants, its presence in the class Hepaticae is comparatively rare. This phenomenon suggests that triterpenoids biosynthesis could be blocked in most liverworts (Asakawa et al., 2012). However, *L. chordulifera* investigations showed that triterpenoids were the major constituents of the plant extract, which is clearly a distinctive feature of this species.

Table 1
^{1}H NMR (300 MHz) and ^{13}C NMR (75 MHz) spectral data of compounds **3**, **4**, and **5** ($CDCl_3$).

	3		**4**		**5**	
	^{1}H	^{13}C	^{1}H	^{13}C	^{1}H	^{13}C
3	3.22 dd (10.5, 5.0)	79.1	3.22 dd (10.9, 4.8)	79.1	3.19 dd (10.8, 5.2)	79.1
12	5.28 t (3.5)	122.7	5.25 t (3.4)	126	1.69 m	25.5
18	2.81 dd (13.7, 4.3)	40.9	2.19 d (11.7)	52,7	1.61 m	49.2
23	0.77 s	28.1	0.78 s	15.8	0.75 s	15.3
24	0.98 s	15.5	0.98 s	28.2	0.96 s	28.1
25	0.91 s	13.3	0.93 s	15.6	0.82 s	16.2
26	0.75 s	17.1	0.79 s	17.3	0.93 s	16
27	1.13 s	26.0	1.08 s	23.9	0.97 s	14.7
28	–	183.1	–	180.9	–	181.2
29	0.90 s	33.1	0.86 d (6.8)	17.0	4.61 s (a), 4.73 s (b)	110.1
30	0.93 s	23.6	0.94 d (6.4)	21.2	1.68 s	19.5

Coupling constants (*J* in Hz) are given in parenthesis.
Signals indicated with *m* were unresolved or overlapping multiplets.
The ^{13}C assignments were confirmed by HSQC, DEPT, and HMBC measurements.

Tests

None of the evaluated compounds displayed neither bacterial growth nor biofilm formation up to 50 μg/ml. Results of effects produced by compounds **2**–**11** against *P. aeruginosa* and *S. aureus* at 50 μg/ml are presented in Figs. 2 and 3, respectively.

Bacterial growth

None of the tested compounds displayed antibacterial activity against *P. aeruginosa* at 50 μg/ml (Fig. 2). Compounds **4**, **5**, **7**–**10** showed bacterial growth increments of 41, 14, 14, 20, 16, and 12%, respectively, when were compared with control growth at the same concentration.

S. aureus bacterial growth was only significantly reduced by compounds **3** and **11** (38 and 22%, respectively, Fig. 3). Compounds **4**, **6**, **7**, **9**, and **10** stimulated bacterial growth by 12, 19, 16, 9, and 12%, respectively, in comparison with control growth. Compounds **2**, **5**, and **8** had no effect.

Biofilm formation

Although compounds **6**–**11** did not inhibit *P. aeruginosa* bacterial growth at 50 μg/ml, they were able to significantly decrease its biofilm formation by 27, 38, 51, 33, 47, and 60%, respectively, in relation to control (Fig. 2). Ciprofloxacin at 5 μg/ml, inhibited 89% the biofilm formation.

S. aureus biofilm formation was inhibited by 45% by ciprofloxacin at 5 μg/ml, while compounds **2**, **6**, **8, 9**, and **11** significantly reduced *S. aureus* biofilm formation by 37, 27, 30, 28, and 38% at 50 μg/ml, respectively (Fig. 3). In contrast, compounds **3**, **4**, and **5** stimulated 30, 33, and 88% the biofilm production, respectively. Compounds **7** and **10** did not significantly modify the biofilm formation.

Quorum sensing process

None of the tested compounds was able to significantly alter the Quorum Sensing process of *P. aeruginosa*. Azithromycin, used as positive control of inhibition of the Quorum Sensing process, reduced 81% the autoinducers production (Fig. 2).

Elastase activity

All the tested compounds were able to significantly decrease the elastase activity of *P. aeruginosa* (Fig. 2). The most potent were the triterpene acids **4** and **5,** reducing 96 and 92% elastase activity, respectively. Compounds **2**, **3**, and **6**–**11** reduced 60, 65, 75, 73, 75, 60, 70, and 55%, respectively, the enzyme activity.

Discussion

Compound **11**, the only aromadendrane tested, was able to inhibit *P. aeruginosa* biofilm formation by 60% and elastase activity by 45% without altering significantly bacterial growth. Similar effects were produced by compound **6** (shoreic acid) inhibiting 27% biofilm formation and 75% elastase activity. Compounds that do not alter bacterial growth do not produce selective pressure over the microorganism that can lead to appearance of resistance. However, microorganisms with their main defense mechanism (biofilm) affected and with one of their main virulence factors attenuated (elastase), might be susceptible to the attack of the host immune system. Compounds able to attenuate virulence factors of

Table 2
^{1}H NMR (300 MHz) spectral data of compounds **6**–**9** ($CDCl_3$).

H	**6**	**7**	**8**	**9**
3	–	–	–	3.40 t (2)
18	0.85 s	0.86 s	1.01 s	0.97 s
19	0.88 s	0.90 s	0.94 s	0.86 s
21	1.11 s	1.35 s	1.15 s	1.15 s
24	3.64 m	–	3.64 dd (9.6, 5.5)	3.65 dd (9.6, 5.4)
26	1.14 s	–	1.19 s	1.19 s
27	1.19 s	–	1.11 s	1.11 s
28	4.65 s (a), 4.84 s (b)	4.66 s (a), 4.86 s (b)	1.08 s	0.94 s
29	1.73 s	1.74 s	1.04 s	0.84 s
30	1.01 s	1.01 s	0.88 s	0.89 s

Coupling constants (*J* in Hz) are given in parenthesis.
Signals indicated with *m* were unresolved or overlapping multiplets.

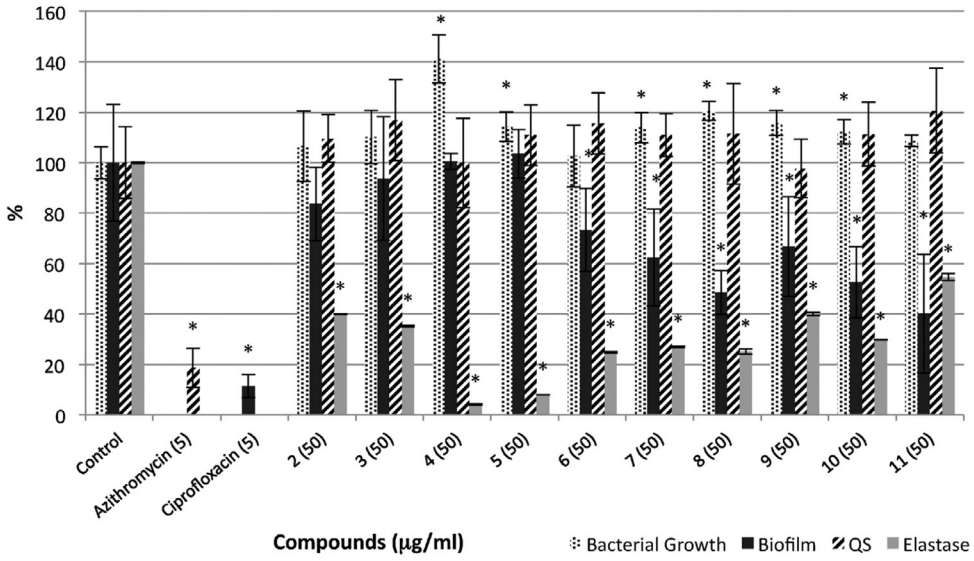

*Significant differences ($p < 0.05$) in comparison with negative control group were detected (Dunnett's test).

Fig. 2. Effects of compounds **2**–**11** at 50 μg/ml and antiobiotics used as positive control at 5 μg/ml (azithromycin for QS and ciprofloxacin for biofilm formation) on bacterial growth, biofilm formation, QS, and elastase activity of *Pseudomonas aeruginosa*. Control values were established as 100%, higher or slower values indicate stimulation or inhibition, respectively. * Significant differences ($p < 0.05$) in comparison with negative control group were detected (Dunnett's test).

microorganisms without altering bacterial growth can be desirable in the postulation of new anti-pathogenic substances.

Despite the triterpenic acids **4** and **5**, did not significant affect the *P. aeruginosa* biofilm formation, they inhibited more than 90% elastase activity. Previous reports indicate that directly or indirectly, LasB as well as other secreted enzymes can influence the formation and architecture of *P. aeruginosa* biofilms as a result of changes in extracellular polymeric substances composition and properties, as well as the motility of the cells (Tielen et al., 2010). LasB inhibition can significantly decrease bacterial attachment, microcolony formation, and extracellular matrix linkage in biofilm (Yu et al., 2014). Bacterial biofilms produced in presence of **4** and **5** despite of not being affected in biomass quantity, they were probably affected in their functionality which clearly means less pathogenic bacteria.

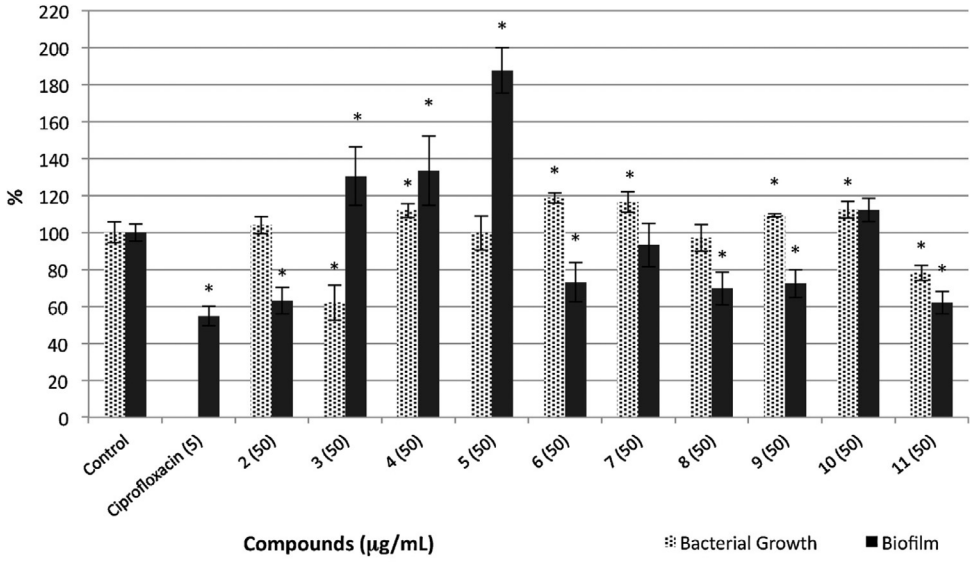

*Significant differences ($p < 0.05$) in comparison with negative control group were detected (Dunnett's test).

Fig. 3. Effects of compounds **2**–**11** at 50 μg/ml and ciprofloxacin at 5 μg/ml (used as positive controls of biofilm formation) on bacterial growth and biofilm formation of *Staphylococcus aureus*. Control values were established as 100%, higher or slower values indicate stimulation or inhibition, respectively. * Significant differences ($p < 0.05$) in comparison with negative control group were detected (Dunnett's test).

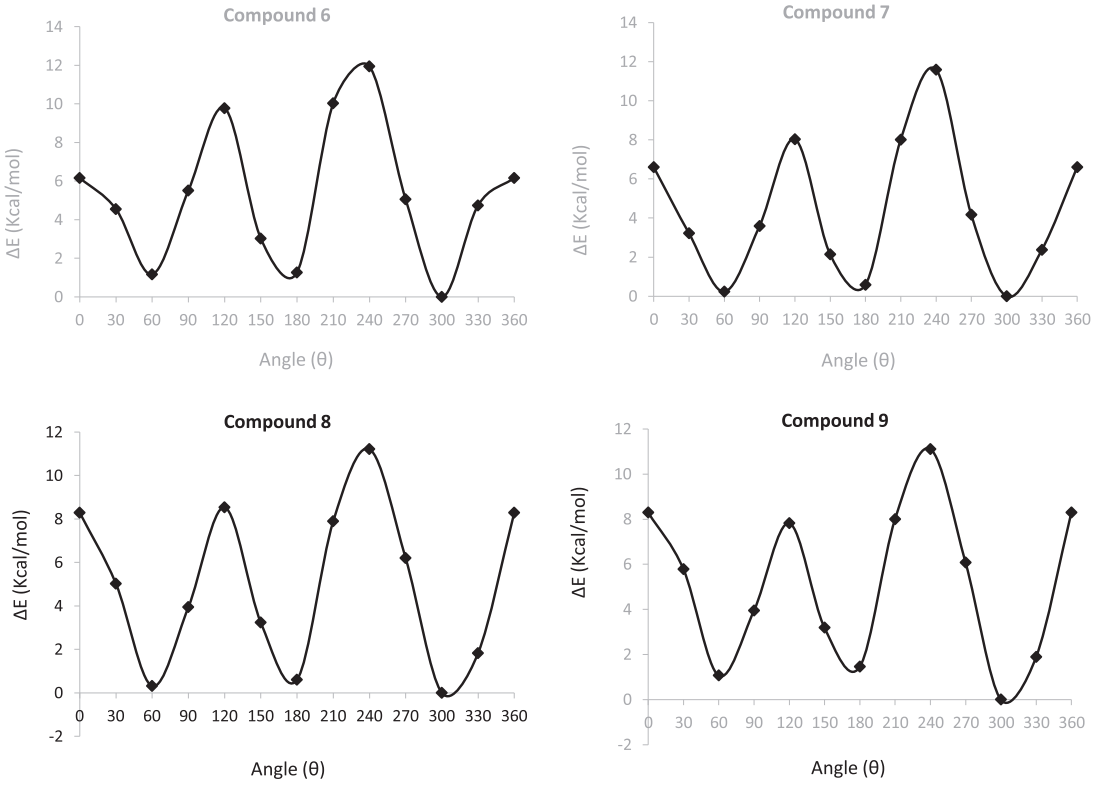

Fig. 4. Potential energy curves (PECs) obtained for the torsional angle θ of compounds **6**, **7**, **8**, and **9**.

Among the tested compounds against *S. aureus*, only the aromadendrane viridiflorol (**11**) was able to inhibit bacterial growth and biofilm formation, while compounds **2** and **8** reduced biofilm formation (37 and 30%, respectively) without altering bacterial growth.

Structure activity relationships (SAR)

Viridiflorol (**11**), the only evaluated sesquiterpenoid, was less active than the triterpenoids **2**–**10** on its ability to control elastase activity of *P. aeruginosa*. However, viridiflorol (**11**) was more potent than the mentioned triterpenoids inhibiting biofilm formation. This antibiofilm activity was previously observed in other aromadendrane sesquiterpenoids from the liverwort *Porella chilensis* (Gilabert et al., 2011).

Among the analyzed triterpenoids, those that posses a dammarane skeleton (**6**–**10**) were the most potent inhibitors of the *P. aeruginosa* biofilm formation. The presence of the THF ring on C-17 (compounds **6**–**9**), the presence of a carbonyl or hydroxyl group on C-3 (compounds **8**–**10**), or the A ring opening (compounds **6** and **7**) appear not to be essential molecular arrangements for the activity. Then, a greater number of related compounds is necessary in order to approach to the minimum requirements.

Regarding the elastase activity, the pentacyclic triterpene acids **4** and **5** were the most active, both carrying a carboxylic acid on C-17. However, despite compound **3** also possesses a carboxylic group on C-17, it is not as active as **4** and **5**. Therefore, the carboxylic group on C-17 is not the only requirement for *P. aeruginosa* elastase activity.

When the bioactive profile of the tested compounds against *S. aureus* is analyzed, it can be seen that the pentacyclic triterpene acids **3**–**5** produced stimulations of biofilm formation, while the pentacyclic triterpene taraxerol (**2**) inhibited it, indicating that the carboxylic group is important for the mentioned stimulation.

The dammarane compounds **6**, **8**, and **9** were able to inhibit *S. aureus* biofilm formation. This seems to indicate that the THF ring on C-17 bonded to an isopropylol group is required for the mentioned activity. In order to investigate the effects of the spatial orientation of the THF ring on the *S. aureus* biofilm production, a computer-assisted conformational and electronic study of the dammarane skeleton was performed.

Potential energy curves (PECs) were obtained by rotating the torsional angle θ (C13–C17–C20–O, Fig. 1) 30° each. PECs calculated for compounds **6**–**9** are given in Fig. 4 in which the influence of the THF ring's orientation on the potential energy of the rotamers is represented. As can be seen, characteristic 3-fold periodicity curves with three low-energy conformations near 60°, 180°, and 300° with interconversion barriers of about 10 kcal/mol were predicted. These high values of energy indicate a low molecular flexibility for this rotation. In addition, geometries of the different low-energy conformations obtained for compounds **6**–**9** were optimized without the application of any kind of restriction to the torsional angle θ. These results are summarized in Table 3. The calculated θ values for the lowest-energy conformer of compounds **6**, **8**, and **9**, corresponding to the global minima in PECs, were near to 310° (308.2, 310.4, and 309.9, respectively), while in compound **7** this angle adopts a value of 305.8.

Once obtained the energetically preferred conformation of compounds, an electronic analysis using molecular electrostatic potentials (MEPs) was performed. Fig. 5 shows the MEPs obtained for the preferred conformation of compound **6**–**9**. The electrostatic potential provides a representative measure of overall molecular charge distribution and offers reliable information about the reactivities of potential interaction sites of the molecules. The MEP maps of compounds **6**, **8**, and **9**, exhibited, in the zone of the THF ring, two clear minima represented as deep red zones ($V(r)$ of about -0.120 el/au^3) located in the proximity of the oxygenated functions. The MEP map of compound **7**, exhibited just one of these

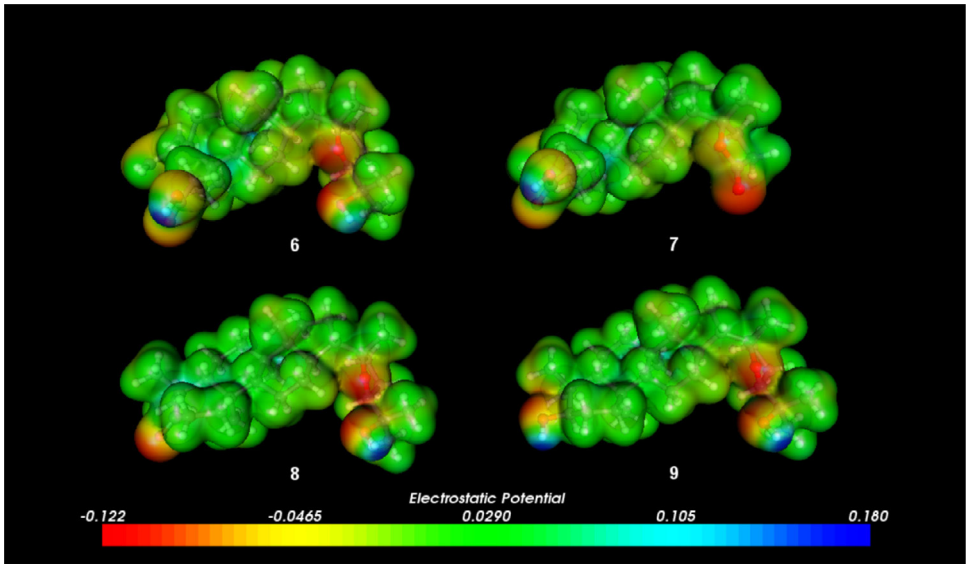

Fig. 5. Molecular electrostatic potential-encoded electron density surfaces of compounds **6**–**9**. Surfaces were generated using B3LYP/6-311G++ (d and p) single point calculations. Coloring represents electrostatic potential with red and blue indicating the electronegative or the electropositive areas, respectively. The color-coded is shown at the bottom, where red is representing the most negative and blue the most positive values, respectively. Intermediate negative and positive values are represented by colors that downgrades from orange to light blue. (For interpretation of the references to color in this figure legend, the reader is referred to the web version of this article.)

deep red zones located in the proximity of the carbonyl group in C-24. In the proximity of the oxygen located between C-20 and C-24 a yellow zone ($V(r)$ of about -0.046 el/au^3) was observed.

The spatial and electronic conformations adopted by compound **7** differ from those adopted by compounds **6**, **8**, and **9**, which share similar spatial and electronic features in the zone of the THF ring. It is possible to rationalize results for the theoretical study as follows; the absence of the isopropylol group leads to compound 7 to adopt an unfavorable electronic and spatial arrangement for the activity since compound **7** displays no activity on *S. aureus* biofilm formation. On the other hand, it is important to point out that all the dammarane compounds, including **7** and **10**, were able to inhibit *P. aeruginosa* biofilm formation, indicating that the bioactivity on *P. aeruginosa* and *S. aureus* occurs via different mechanisms.

Regarding the pentacyclic triterpenes **2**–**5**, as it was previously mentioned, only compound **2** was able to inhibit *S. aureus* biofilm formation, **3**–**5** produced stimulations, and **1** was not tested. Then, the electronic and spatial profiles of compounds **1**–**5** was investigated following the procedure described above. Once obtained the optimized structures of compounds, an electronic analysis using molecular electrostatic potentials (MEPs) were performed (Fig. 6).

Table 3
Angles and energy values obtained for the low-energy conformations of compounds **6**–**9**. Optimizations were performed using DFT [B3LYP/6-31G(d)] calculations.

Compound	Angle (θ)	ΔE (kcal/mol)
6	63.2	1.05
	170.4	0.77
	308.2	0.00
7	63.4	0.62
	163.7	0.71
	305.8	0.00
8	64.1	0.87
	172.5	1.28
	310.4	0.00
9	64.2	0.87
	172.7	1.15
	309.9	0.00

As can be seen, compound **2** presents a deep red electronegative zone around the hydroxyl group (left side of molecule) and a second one in de vicinity of C-14 due to the presence of a double bound which shares electron density. Despite the fact that compounds **2**–**4** show almost identical spatial and electronic configurations on the zone of the hydroxyl group, compounds **3** and **4** present a strong electronegative zone near to the carboxylic group (right side). These hydrophilic zones could interfere with the hypothetical ligand-receptor interactions related to the activity. Compound **5**, presents two electronegative zones near to the oxygenated funtions also, and differs from **3** and **4** in its spatial orientation. It is important to note that compound **5** not only shows the most important differences with **2** in its electronic and spatial profile but also in the activity, being **5** the most active *S. aureus* biofilm formation stimulator of the series. On the other hand, compound **1** shows almost identical profiles to **2** in the vecinity of the hydroxyl group and in the proximity of C-14. Unfortunately, since compound **1** underwent partial decomposition it couldn't be tested.

Some of the *L. chordulifera* compounds showed promissing activities against two common human pathogenic bacteria and the performed SAR study allowed in some cases approaching to the minimum requirements for biological activities. More studies are necessary to further characterize the complete anti-pathogenic profile of these terpenoids and the involved mechanisms of action.

Compounds

Taraxerone (**1**) 1*H* NMR ($CDCl_3$, 300 MHz): δ 5.56 (1*H*, dd, $J = 8.1$, 3.2 Hz, H-15), 1.14 (3*H*, s, H-27), 1.09 (3*H*, s, H-23), 1.08 (3*H*, s, H-25), 1.07 (3*H*, s, H-24), 0.96 (3*H*, s, H-29), 0.92 (3*H*, s, H-28), 0.91 (3*H*, s, H-30), 0,83 (3*H*, s, H-26).

Taraxerol (**2**) 1*H* NMR ($CDCl_3$, 300 MHz): δ 5.53 (1*H*, dd, $J = 3.2$, 8.2 Hz, H-15), 3.24 (1*H*, dd, $J = 5.0$, 10.5 Hz, H-3), 1.09 (3*H*, s, H-26), 0.98 (3*H*, s, H-23), 0.95 (3*H*, s, H-29), 0.92 (3*H*, s, H-25), 0.90 (3*H*, s, H-27), 0.90 (3*H*, s, H-30), 0.82 (3*H*, s, H-28), 0.80 (3*H*, s, H-24).

3ß-hydroxynordammaran-20-one (**10**) 1*H* NMR ($CDCl_3$, 300 MHz): δ 3.20 (1*H*, dd, $J = 5.4$, 10.9 Hz, H-3), 2.58 (1*H*, td, $J = 6.1$, 10.9 Hz, H-17), 2.13 (3*H*, s, H-21), 0.98 (3*H*, s, H-18), 0.97 (3*H*, s, H-29), 0.87 (3*H*, s, H-30), 0.84 (3*H*, s, H-19), 0.77 (3*H*, s, H-28).

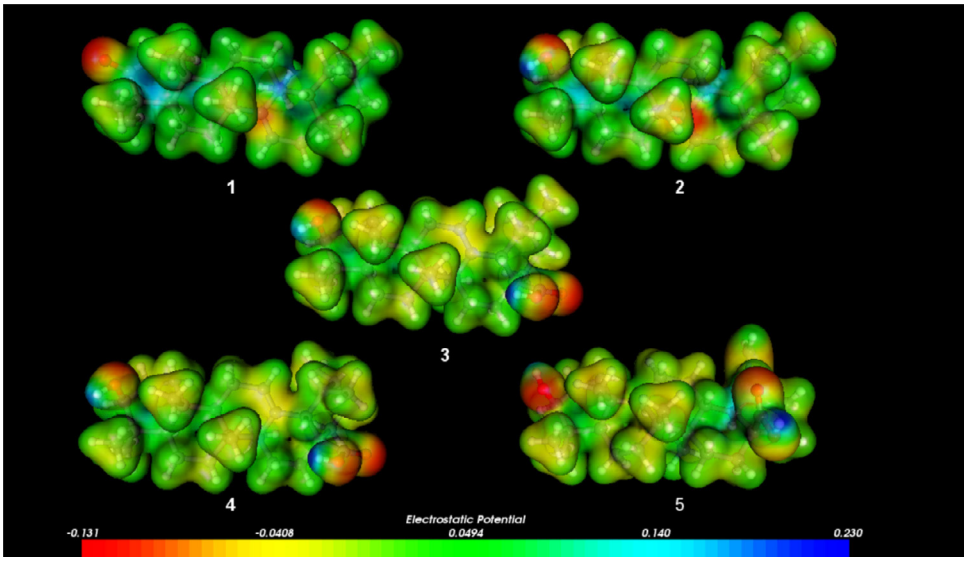

Fig. 6. Molecular electrostatic potential-encoded electron density surfaces of compounds **1**–**5**.

Viridiflorol (**11**) 1*H* NMR ($CDCl_3$, 300 MHz): δ 1.15 (3*H*, s, H-14), 1.02 (3*H*, s, H-12), 1.00 (3*H*, s, H-13), 0.92 (3*H*, d, $J = 6.5$ Hz, H-15), 0.61 (1*H*, td, $J = 10.3$, 5.8 Hz, H-7), 0.11 (1*H*, t, $J = 9.0$ Hz, H-6).***ent*-Spathulenol** (**12**) 1*H* NMR ($CDCl_3$, 300 MHz): δ 4.69 (1*H*, s, H-14a), 4.67 (1*H*, s, H-14b), 2.42 (2*H*, dd, $J = 13.3$, 6.0 Hz, H-9), 1.28 (3*H*, s, H-15), 1.06 (3*H*, s, H-13), 1.04 (3*H*, s, H-12), 0.47 (1*H*, dd, $J = 11.2$, 9.4 Hz, H-6).

Conflict of interest: All authors have no conflict of interest to disclose.

Acknowledgments

This work was supported by grants from ANPCyT, (PICT 2011 No 1202) CONICET, and CIUNT, (26D/410, 26D/407), Argentina.

References

Amaya, S., Pereira, J.A., Borkosky, S., Valdez, J.C., Bardon, A., Arena, M.E., 2012. Inhibition of quorum sensisng on *Pseudomonas aeruginosa* by sesquiterpene lactones. Phytomedicine 19, 1173–1177.

Ardiles, V., Cuvertino, J., Osorio, F., 2008. Briófitas de los bosques templados de Chile. Corporación Chilena de la Madera, Concepción.

Arena, M.E., Cartagena, E., Gobbato, N., Baigori, M., Valdez, J.C., Bardon, A., 2011. In vivo and in vitro antibacterial activity of acanthospermal B, a sesquiterpene lactone isolated from *Acanthospermum hispidum*. Phytother. Res. 25, 597–602.

Asakawa, Y., Ludwiczuk, A., Nagashima, F., Kinghorn, A.D., Falk, H., Kobayashi, J., 2012. Chemical Constituents of Bryophytes: Bio- and Chemical Diversity, Biological Activity, and Chemosystematics. Springer, Vienna.

Ayatollahi, A.M., Ghanadian, M., Afsharypour, S., Abdella, O.M., Mirzai, M., Askari, G., 2011. Pentacyclic triterpenes in *Euphorbia microsciadia* with their t-cell proliferation activity. Iran. J. Pharm. Res. 10, 287–294.

Bombarda, I., Raharivelomanana, P., Ramanoelina, P.A.R., Faure, R., Bianchini, J.P., Gaydou, E.M., 2001. Spectrometric identifications of sesquiterpene alcohols from niaouli (*Melaleuca quinquenervia*) essential oil. Anal. Chim. Acta 447, 113–123.

Caballero, A.R., Moreau, J.M., Engel, L.S., Marquart, M.E., Hill, J.M., O'Callaghan, R.J., 2001. *Pseudomonas aeruginosa* protease IV enzyme assays and comparison to other *Pseudomonas proteases*. Anal. Biochem. 290, 330–337.

Cartagena, E., Colom, O.A., Neske, A., Valdez, J.C., Bardón, A., 2007. Effects of plant lactones on the production of biofilm of *Pseudomonas aeruginosa*. Chem. Pharm. Bull. 55, 22–25.

Cathcart, G.R., Gilmore, B.F., Greer, B., Harriott, P., Walker, B., 2009. Inhibitor profiling of the *Pseudomonas aeruginosa* virulence factor LasB using N-alpha mercaptoamide template-based inhibitors. Bioorg. Med. Chem. Lett. 19, 6230–6232.

Costerton, J.W., Stewart, P.S., Greenberg, E.P., 1999. Bacterial biofilms: a common cause of persistent infections. Science 284, 1318–1322.

Flegel, M., Becker, H., 1999. Di- and triterpenoids from the liverwort *Blepharidophyllum densifolium*. Z. Naturforsch. C 54, 481–487.

Gilabert, M., Ramos, A.N., Schiavone, M.M., Arena, M.E., Bardón, A., 2011. Bioactive sesqui- and diterpenoids from the argentine liverwort *Porella chilensis*. J. Nat. Prod. 74, 574–579.

Gohari, A.R., Saeidnia, S., Hadjiakhoondi, A., Abdoullahi, M., Nezafati, M., 2009. Isolation and quantificative analysis of oleanolic acid from *Satureja mutica* Fisch & C.A Mey. J. Med. Plants 8, 65–69.

Govindachari, T.R., Suresh, G., Kumari, G.N.K., 1994. Triterpenoids from *Dysoxylum malabaricum*. Phytochemistry 37, 1127–1129.

Güvenalp, Z., Özbek, H., Kuruüzüm-Uz, A., Kazaz, C., Demirezer, L.O., 2009. Secondary metabolites from *Nepeta heliotropifolia*. Turk. J. Chem. 33, 667–675.

Hernandez-Chavez, I., Torrez-Tapia, L.W., Sima-Polanco, P., Cedillo-Rivera, R., Moo-Puc, R., Peraza-Sanchez, S.R., 2012. Antigiardial activity of *Cupania dentata* bark and its constituents. J. Mex. Chem. Soc. 56, 105–108.

Hisham, A., Ajitha Bai, M.D., Fujimoto, Y., Hara, N., Shimada, H., 1996. Complete ^{1}H and ^{13}C NMR spectral assignment of cabraleadiol, a dammarane triterpene from *Dysoxylum malabaricum* bedd. Magn. Reson. Chem. 34, 146–150.

Liu, P.V., 1974. Extracellular toxins of *Pseudomonas aeruginosa*. J. Infect. Dis. 130, S94–S99.

Morales-Serna, J.A., García-Ríos, E., Madrigal, D., Cárdenas, J., Salmón, M., 2011. Constituents of organic extracts of *Cuphea hyssopifolia*. J. Mex. Chem. Soc. 55, 62–64.

Muhit, M.A., Tareq, S.M., Apu, A.S., Basak, D., Islam, M.S., 2010. Isolation and identification of compounds from the leaf extract of *Dillenia Indica* Linn. Blang. Pharm. J. 13, 49–53.

O'Toole, G.A., Kolter, R., 1998. Flagellar and twitching motility are necessary for *Pseudomonas aeruginosa* biofilm development. Mol. Microbiol. 30, 295–304.

Politzer, P., Truhlar, D., 1981. Chemical Applications of Atomic and Molecular Electrostatic Potentials: Reactivity, Structure, Scattering, and Energetics of Organic, Inorganic, and Biological Systems. Plenum Publishing, New York, NY.

Sandasi, M., Leonard, C.M., van Vuuren, S.F., Viljoen, A.M., 2011. Peppermint (*Mentha piperita*) inhibits microbial biofilms in vitro. S. Afr. J. Bot. 77, 80–85.

Singh, Y., Aalbersberg, W., 1992. Dammarane triterpenoids from *dysoxylum richii*. Phytochemistry 31, 4033–4035.

Socolsky, C., Arena, M.E., Asakawa, Y., Bardón, A., 2010. Antibacterial prenylated acylphloroglucinols from the Fern *Elaphoglossum yungense*. J. Nat. Prod. 73, 1751–1755.

Sokol, P.A., Kooi, C., Hodges, R.S., Cachia, P., Woods, D.E., 2000. Immunization with a *Pseudomonas aeruginosa* elastase peptide reduces severity of experimental lung infections due to *P. aeruginosa* or *Burkholderia cepacia*. J. Infect. Dis. 181, 1682–1692.

Stewart, P.S., Costerton, J.W., 2001. Antibiotic resistance of bacteria in biofilms. Lancet 358, 135–138.

Tanaka, R., atsuda, M., atsunaga, S., 1987. 3ß-Hydroxyhexanordammaran-20-one from *Euphorbia supina*. Phytochemistry 26, 3365–3366.

Tateda, K., Comte, R., Pechere, J.C., Köhler, T., Yamaguchi, K., van Delden, C., 2001. Azithromycin inhibits quorum sensing in *Pseudomonas aeruginosa*. Antimicrob. Agents Chemother. 45, 1930–1933.

Tielen, P., Rosenau, F., Wilhelm, S., Jaeger, K.E., Flemming, H.C., Wingender, J., 2010. Extracellular enzymes affect biofilm formation of mucoid *Pseudomonas aeruginosa*. Microbiology 156, 2239–2252.

van Delden, C., Iglewski, B.H., 1998. Cell-to-cell signaling and *Pseudomonas aeruginosa* infections. Emerg. Infect. Dis. 4, 551–560.

Whiteley, M., Lee, K.M., Greenberg, E.P., 1999. Identification of genes controlled by quorum sensing in *Pseudomonas aeruginosa*. Proc. Natl. Acad. Sci. U.S.A. 96, 13904–13909.

Yu, H., He, X., Xie, W., Xiong, J., Sheng, H., Guo, S., Huang, C., Zhang, D., Zhang, K., 2014. Elastase LasB of *Pseudomonas aeruginosa* promotes biofilm formation partly through rhamnolipid-mediated regulation. Can. J. Microbiol. 60, 227–235.

Zapp, H., Orth, K., Zapp, J., Connolly, J.D., Becker, H., 2008. 21,28-Epoxy-18ß,21ß-dihydroxbaccharan-3-one and other terpenoids from the liverwort *Lepidozia chordulifera* T. Taylor. Nat. Prod. Comun. 3, 1755–1758.

Zhang, Y.L., 2011. Chemical Constituents of Liverworts *Lepidozia reptans* and *Asterella multiflora*. Shandong University, China (Master thesis).